PERGAMON

International Journal of Multiphase Flow 27 (2001) 1829–1858

International Journal of Multiphase Flow

www.elsevier.com/locate/ijmulflow

Validation of a stochastic Lagrangian modelling approach for inter-particle collisions in homogeneous isotropic turbulence

Martin Sommerfeld *

Institut für Verfahrenstechnik, Fachbereich Ingenieurwissenschaften, Martin-Luther-Universität Halle-Wittenberg, D-06099 Halle (Saale), Germany

Received 30 March 2000; received in revised form 3 May 2001

Abstract

A stochastic inter-particle collision model for particle-laden flows to be applied in the frame of the Euler/Lagrange approach is introduced. The model relies on the generation of a fictitious collision partner with a given size and velocity, whereby no information is required on the actual position and direction of motion of the surrounding real particles. However, the fictitious particle is a representative of the local particle phase properties. In sampling the velocity of the fictitious particle correlation with the velocity of the real particle as a consequence of turbulence is accounted for. The occurrence of a collision is decided based on the collision probability according to kinetic theory. For validating the collision model, results from large eddy simulations (LES) are used for monodisperse particles being dispersed in a homogeneous isotropic turbulence and a binary mixture of particles. In the case of the binary mixture two situations are considered; a granular medium without particle-flow interaction and two fractions of particles settling under the action of gravity in an isotropic homogeneous turbulence. For all the considered test cases the agreement of the model calculations with the results obtained by LES was found to be very good.

Keywords: Gas–solid flows; Binary mixture; Turbulence; Euler/Lagrange approach; Inter-particle collisions; Inelastic collisions; Stochastic collision model

1. Introduction

Turbulent gas–solid flows with high particle loading are frequently found in technical and industrial processes. Examples are pneumatic conveying, fluidised beds, vertical risers, particle

* Tel.: +49-3461-462-879; fax: +49-3461-462-878.
E-mail address: martin.sommerfeld@iw.uni-halle.de (M. Sommerfeld).

0301-9322/01/$ - see front matter
PII: S0301-9322(01)00035-0

separation in cyclones, mixing devices, and others. In such particle-laden flows the particle behaviour may be considerably affected by inter-particle collisions in addition to aerodynamic transport and turbulence effects if the mass loading is high or regions of high concentration develop as a result of inertial effects (Sommerfeld, 1995). Quite a number of theoretical studies on the collision rate of particles or droplets in turbulent flows have been published in the past. A detailed review was given for example by Williams and Crane (1983) and Pearson et al. (1984). Recently, also the method of direct numerical simulation (DNS) is being extensively used for the analysis of inter-particle collisions mainly in isotropic turbulent flows applying a particle tracking approach with point-particles (Sundaram and Collins, 1997; Wang et al., 1998; Zhou et al., 1998; Mei and Hu, 1999). The most realistic collision scheme in these studies was used by Sundaram and Collins (1997) who utilised hard sphere collisions similar to the present study, as will be demonstrated below. In all other publications somewhat artificial collision schemes are applied. Some of them are closer to describe an agglomeration process, as for example the "throw away" model of Mei and Hu (1999). In the DNS studies of Wang et al. (1998) and Zhou et al. (1998) several different collision schemes were tested, all of which are not very realistic with regard to the application in technical systems (Mei and Hu, 1999). However, in some cases the particle volume concentration is so low that one may assume that the post-collision treatment has no strong effect on the derived collision statistics (Mei and Hu, 1999).

In turbulent flows two limiting cases may be identified by using a particle Stokes number which is defined as the ratio of particle response time, τ_p, to the relevant time scale of turbulence, T_t

$$St = \frac{\tau_p}{T_t}. \tag{1}$$

In the present work, the integral time scale of turbulence is most suitable, since rather inertial particles with respect to the dissipation scales of turbulence are considered. For particles which are small compared with the Kolmogorov length scale, and completely follow the turbulence (i.e. $St \to 0$), Saffman and Turner (1956) provided an approximate expression for the collision rate of droplets in atmospheric turbulence. The collision rate (i.e. collisions per unit volume and time) for two droplet size classes with the radii $R_{p,i}$ and $R_{p,j}$ and with the number concentrations $n_{p,i}$ and $n_{p,j}$ (i.e. particles per unit volume) is given by

$$N_{ij} = \left(\frac{8\pi}{15}\right)^{1/2} n_{p,i}\, n_{p,j} (R_{p,i} + R_{p,j})^3 \left(\frac{\varepsilon}{\nu}\right)^{1/2}, \tag{2}$$

where ϵ is the dissipation rate of turbulent energy and ν is the kinematic viscosity. Hence, for this limiting case the collision rate depends solely on droplet size, concentration and the local velocity gradient and therefore is called collision rate due to isotropic turbulent shear.

The other limiting case is the kinetic theory for $St \to \infty$, where the particle motion is completely uncorrelated with the fluid and hence the velocity of colliding particles is also uncorrelated. This case was analysed by Abrahamson (1975) for heavy particles in high intensity turbulence neglecting external forces, which implies that there is no mean drift between the particles. The resulting collision rate between two particle classes is given by

$$N_{ij} = 2^{3/2}\, \pi^{1/2}\, n_{p,i}\, n_{p,j} (R_{p,i} + R_{p,j})^2 \sqrt{\sigma_{p,i}^2 + \sigma_{p,j}^2}, \tag{3}$$

where σ_p is the mean fluctuating velocity of the particles assuming that all components are identical (i.e. isotropic fluctuating motion $\sigma_p^2 = \overline{u_p'^2} = \overline{v_p'^2} = \overline{w_p'^2}$). In practical two-phase flows the two limits are rarely met, rather the particles may partially respond to turbulence. Hence, the velocities of colliding particles will be correlated to a certain degree, since they are transported in the same turbulent eddy upon collision. The degree of correlation depends on the turbulent Stokes number defined above (Eq. (1)). An analysis of this effect was performed by Williams and Crane (1983) and an expression for the collision rate of particles in turbulent flows covering the entire range of particle Stokes numbers and accounting for a possible correlation of the velocities of colliding particles was suggested. The expression for the collision rate is given in terms of particle concentration, particle relaxation times (i.e. Stokes numbers), turbulence intensities, and turbulent scales.

$$N_{ij} = (162\pi)^{1/2} n_{p,i} n_{p,j} \nu L_t \frac{\rho}{\rho_p} \frac{\overline{u_{rel}}}{\sigma_F} (St_i^{0.5} + St_j^{0.5})^2 \frac{2}{\pi} \times \tan^{-1} \left\{ \frac{1}{3} \frac{\rho_p}{\rho} \frac{\sigma_F L_t}{\nu} \left(\frac{\overline{u_{rel}}}{\sigma_F} \right)^2 \frac{St_i St_j}{(St_i^{0.5} + St_j^{0.5})^2} \right\}. \tag{4}$$

Here L_t is the integral length scale of turbulence, $\overline{u_{rel}}$ the mean relative velocities between colliding particles, σ_F the fluctuating velocity of the fluid assuming isotropic turbulence, and ρ and ν are the density and the kinematic viscosity of the fluid. The Stokes numbers of the two particle classes are defined in terms of the integral time scale of turbulence. A universal solution for the mean relative velocity between the particles was determined by fitting the results for small and large Stokes numbers and is given by Williams and Crane (1983)

$$\frac{\overline{u_{rel}^2}}{\sigma_F^2} = \frac{(St_i + St_j)^2 - 4 St_i St_j \left\{ \frac{(1+St_i+St_j)}{(1+St_i)(1+St_j)} \right\}^{1/2}}{(St_i + St_j)(1 + St_i)(1 + St_j)}. \tag{5}$$

A similar expression which accounts for the correlated motion of particles was introduced by Kruis and Kusters (1997). However, their analysis accounts for the added mass term which becomes for example important for liquid–solid systems. However, in the present case (i.e. solid particles in air) the resulting additional terms reduce to unity due to the large ratio of turbulent integral time scale to the Kolmogorov time scale.

Modelling of inter-particle collisions in the frame of the Euler/Lagrange method for the numerical calculation of two-phase flows has been based so far mainly on two approaches: a direct simulation and a model based on concepts of the kinetic theory of gases. The most straightforward approach to account for inter-particle collisions is the direct simulation approach. This requires that all the particles have to be tracked simultaneously through the flow field. Thereby, the occurrence of collisions between any pair of particles can be judged based on their positions and relative motion during one time step. Once a collision occurs the change in translational and angular particle velocities can be determined by solving the equations for the conservation of linear and angular momentum in connection with Coulomb's law of friction. When the duration of the collision process is negligibly small compared to the time of collisionless motion, the size of the colliding particles is not too different, and the ratio of solid particle density to the fluid density

is much larger than unity, fluid dynamic effects during the collision process can be neglected and the collision efficiency may be assumed as 100%. This assumption was also made in the present study, however in a recent work the presented stochastic collision model was extended in order to account for a reduced collision efficiency when the colliding particles have a considerable difference in size (Ho and Sommerfeld, 2001).

A direct simulation method of inter-particle collisions was for example applied by Tanaka and Tsuji (1991) for the calculation of vertical gas-particle flow. This calculation was feasible only by considering a relatively short element of a pipe and applying periodic boundary conditions. Furthermore, rather coarse particles were considered (i.e. particle diameters of 0.4 and 1.0 mm), whereby the number of particles for a given mass loading was relatively small and hence only about 1000 particles had to be tracked simultaneously through the flow field. When more complex flow configurations and smaller particles are considered, a direct simulation of inter-particle collisions is not feasible due to the high computational effort and the large storage requirements. Nevertheless, the results of Tanaka and Tsuji (1991) showed a very interesting effect, namely that the particle velocity fluctuations become increasingly isotropic with increasing particle mass loading and hence increasing collision frequency.

The consideration of inter-particle collisions in the most commonly applied Lagrangian approach where one particle is tracked after the other through the flow field requires the derivation of an appropriate collision model, since no information is available about neighbouring particles. Recently, Sommerfeld and Zivkovic (1992) and Oesterle and Petitjean (1993) developed independently a similar stochastic particle–particle collision model which was based on the calculation of the collision probability along the particle trajectory in analogy with kinetic theory of gases. From the value of the collision probability it was decided whether a collision takes place or not. In case a collision occurs a fictitious second particle was generated according to the local probability density functions of particle diameter and velocities. By solving the conservation equations for linear and angular momentum the post-collision velocities of the considered particle were calculated. The post-collision properties of the fictitious particle were not of further interest in the calculations.

In the inter-particle collision model of Oesterle and Petitjean (1993) a Maxwellian distribution function of the relative velocity between the particles was assumed and it was defined as the difference of the instantaneous velocity of the considered particle and the particle mean velocity in the control volume associated with the particle position which is somewhat inconsistent. Moreover, the particle size distribution was not considered in the model of Oesterle and Petitjean (1993). In the inter-particle collision model introduced by Sommerfeld and Zivkovic (1992) the velocity distribution function and the mean relative velocity were determined by the integration according to Abrahamson (1975). The particle size distribution was considered by introducing a log-normal distribution function into the collision probability.

Calculations performed by Sommerfeld and Zivkovic (1992) and Oesterle and Petitjean (1993) demonstrated that inter-particle collisions have a strong influence on the profile of the particle concentration in a developed horizontal gas-particle channel flow, even at a particle mass loading well below unity.

A detailed numerical analysis of the effect of inter-particle collisions on the properties of developed particle-laden horizontal channel flows was also performed by Burmester De Bessa Ribas et al. (1980) and Lourenco et al. (1983) using the Boltzmann statistical method. Moreover, the

influence of the particle phase on the gas flow was considered and the resulting deformation of the gas velocity profile with increasing particle mass loading was demonstrated. The results furthermore revealed that the particle fluctuating motion in the streamwise direction is reduced with increasing particle mass loading and hence increasing collision frequency between the particles. These observations were in agreement with experimental results. Also in these studies rather large particles were considered whereby the influence of turbulence on particle motion could be neglected.

So far in most of the modelling approaches to account for inter-particle collisions in the Euler/Lagrange approach, the correlation of the velocities of colliding particles was not respected. In the present paper a stochastic inter-particle collision model is presented which accounts for the correlation effect (Sommerfeld, 1999). At present however, the model will be restricted to relatively large and inertial particles with respect to the dissipation scales of turbulence, as found in a number of technical applications, as for example pneumatic conveying. Additionally, it is assumed that the size of the particles is not too different whereby the hydrodynamic interaction may be neglected, resulting in a 100% collision efficiency. This implies that the relevant collision mechanism in the considered test cases is turbulent inertia and differential settling. As a result of this fact, one may use large eddy simulations (LES) for validation, since the particle motion is dominantly controlled by the most energetic turbulent eddies. This implies a particle response time which is not very much smaller than the integral time scale of turbulence. In Section 2 an estimation of the importance of inter-particle collisions in gas-particle flows will be presented. Thereafter (Section 3), the assumptions for the fluid flow and the particle tracking approach will be introduced. For the latter the applied model for generating the fluid velocity along the particle trajectory is of great importance. The developed stochastic inter-particle collision model is introduced in Section 4. The model calculations are validated based on data obtained by LES for three test cases:

- Monosized particles dispersed in a isotropic homogeneous turbulence without considering gravity are considered in Section 5 (Lavieville et al., 1995).
- A binary mixture of particles without particle-fluid interaction (i.e. a dry granular medium) and without gravity is considered in Section 6 (Gourdel et al., 1998). In this case the particle motion is solely induced by inter-particle collisions.
- A binary mixture settling under gravity in a isotropic homogeneous turbulence (Gourdel et al., 1998, Gourdel et al., 1999) is also analysed in Section 6.

It should be noted at this point that for the case of monodisperse particles in homogeneous turbulence the effect of preferential concentration (Sundaram and Collins, 1997) was also observed in the LES for the smaller Stokes numbers. For the binary mixture, there was no measurable effect of preferential concentration. The introduced inter-particle collision model however does not explicitly account for this physical phenomenon.

2. Importance of inter-particle collisions

In the following the importance of inter-particle collisions on the development of fluid-solid flows is discussed. The inter-particle collision probability depends mainly on the particle concentration, the particle size, and the fluctuating motion of the particles. A classification of

particle-laden flows in terms of the importance of inter-particle collisions may be based on the ratio of particle response time τ_p to the averaged time between collisions τ_c (Crowe, 1981). In dilute two-phase flows the particle motion will be mainly governed by fluid dynamic transport effects, i.e. drag force, lift forces, and turbulence. On the other hand dense flows are characterised by high collision frequencies between particles and hence their motion is dominantly influenced by inter-particle collisions. Fluid dynamic transport effects are of minor importance. Therefore the two regimes are characterised by the following time scale ratios:

- dilute two-phase flow:

$$\frac{\tau_p}{\tau_c} < 1, \tag{6}$$

- dense two-phase flow:

$$\frac{\tau_p}{\tau_c} > 1. \tag{7}$$

This implies that in dense two-phase flows the time between particle–particle collisions is smaller than the particle response time, whereby the particles are not able to completely respond to the fluid flow between successive collisions. This regime may occur when either very large particles at a low number density are present in the flow or in the case of small particles when the number density is large. In dilute two-phase flows collisions between particles may also occur and influence the flow development to a certain degree, but the time between successive inter-particle collisions is larger than the particle response time, whereby the fluid dynamic transport of the particles is the dominant transport effect.

In the following section an estimate of the boundary between the two regimes will be given for turbulent particle-laden flows. The average time between successive inter-particle collisions results from the average collision frequency

$$\tau_c = \frac{1}{f_c}. \tag{8}$$

The collision frequency of one particle (i.e. $n_{p,i} = 1$) with diameter $D_{p,i}$ and velocity $\vec{u}_{p,i}$ with all other particle classes (i.e. N_{class}) with diameter $D_{p,j}$ and velocity $\vec{u}_{p,j}$ can be calculated according to kinetic theory of gases from

$$f_c = \frac{N_c}{n_{p,i}} = \sum_{j=1}^{N_{class}} \left\{ \frac{\pi}{4} (D_{p,i} + D_{p,j})^2 |\vec{u}_{p,i} - \vec{u}_{p,j}| n_{p,j} \right\}, \tag{9}$$

where N_c is the total number of collisions of particle i with all other particles and $\pi/4(D_{p,i} + D_{p,j})^2$ is the collision cross-section, respectively. The main assumptions associated with the use of Eq. (9) are the following:

- The particle number concentration is small enough that the occurrence of binary collisions prevails.
- On the other hand the particle number concentration must be large enough to allow a statistical treatment.
- The velocities of the colliding particles are not correlated.

An analytic solution of Eq. (9) is only possible for relatively simple cases. For the estimation of the collision frequency, the derivation of Abrahamson (1975) is followed, yielding a collision rate solely determined by turbulence (i.e. the resulting fluctuating motion of the particles) as given by Eq. (3). Furthermore, a monodisperse particle phase is considered, whereby the mean fluctuating velocity is a constant. Hence the collision frequency is obtained as a function of the particle diameter D_p, the total particle number concentration n_p and the mean fluctuating velocity of the particles σ_p

$$f_c = 4\pi^{1/2} n_p D_p^2 \sigma_p. \tag{10}$$

Introducing the volume fraction of the particles $\alpha = \pi/6 D_p^3 N_p$, one obtains after some rearrangements

$$f_c = \frac{24}{\pi^{1/2}} \frac{\alpha \sigma_p}{D_p} \tag{11}$$

or similarly the collision frequency can be expressed as a function of the mass loading $\eta = \dot{m}_p/\dot{m}$, which is often used to characterise gas–solid flows:

$$f_c = \frac{24}{\pi^{1/2}} \frac{\rho}{\rho_p} \frac{\eta \sigma_p}{D_p}. \tag{12}$$

By introducing now the collision frequency and the particle response time (i.e. the Stokesian response time $\tau_p = \rho_p D_p^2/18\mu$) into Eq. (6) the limiting particle diameter for a dilute two-phase flow can be determined as a function of volume fraction or mass loading, respectively:

$$\begin{aligned} D_p &< \frac{3}{4}\pi^{1/2} \frac{\mu}{\alpha \rho_p \sigma_p}, \\ D_p &< \frac{3}{4}\pi^{1/2} \frac{\mu}{\eta \rho \sigma_p}. \end{aligned} \tag{13}$$

Considering a gas–solid flow with the properties ($\rho = 1.15$ kg/m^3, $\rho_p = 2500$ kg/m^3, $\mu = 18.4 \times 10^{-6}$ kg/m s) the limiting particle diameter which separates dilute and dense two-phase flows is calculated as a function of volume fraction and mass loading with the particle velocity fluctuation as a parameter. The result is given in Fig. 1 where the dilute two-phase flow is the domain left of the individual lines and the dense flow regime is on the right-hand side. With increasing particle diameter associated with higher particle inertia, the range of dilute flows is shifted towards lower volume fractions and mass loading. With increasing velocity fluctuation of the particles the boundary line between dilute and dense two-phase flow is shifted to the left, i.e. to smaller mass loading of the dispersed phase. From Eq. (12) it is obvious that the collision frequency increases with the velocity fluctuation.

3. Fluid flow and particle tracking

In the three test cases considered here, the flow field, i.e. turbulence intensities and turbulence length and time scales are prescribed according to the LES. The mean continuous phase velocity is

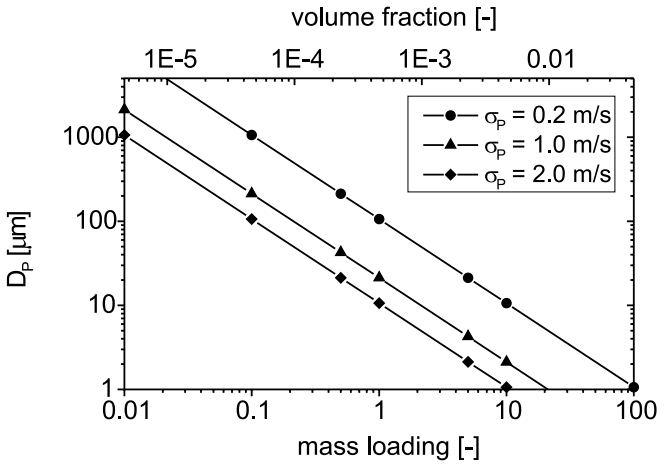

Fig. 1. Regimes of dilute and dense gas–solid flows in dependence of mass loading (and volume fraction) and particle diameter for different particle velocity fluctuations ($\rho = 1.15$ kg/m^3, $\rho_p = 2500$ kg/m^3, $\mu = 18.4 \times 10^{-6}$ kg/(m s)).

zero in both cases. In order to solely assess the effects of inter-particle collisions, two-way coupling effects are not considered in all the test cases. The particle trajectories are calculated sequentially and the particle phase properties are ensemble averaged for each control volume in the computational domain. This approach is possible, since only the steady-state situation is of interest. The present approach may be however also applied if a simultaneous tracking approach is adopted. The forces which are considered in the equation of motion for the particles are the drag and gravity forces only. Hence the following ordinary differential equations are solved along the particle trajectory for the three components of the particle location vector and the particle velocity vector:

$$\begin{aligned} \frac{\mathrm{d}x_{\mathrm{p},i}}{\mathrm{d}t} &= u_{\mathrm{p},i}, \\ \frac{\mathrm{d}u_{\mathrm{p},i}}{\mathrm{d}t} &= \frac{3}{4}\frac{\rho}{\rho_{\mathrm{p}} D_{\mathrm{p}}} c_D (u_i - u_{\mathrm{p},i}) |\vec{u} - \vec{u}_{\mathrm{p}}| + g_i. \end{aligned} \tag{14}$$

For the drag coefficient the following correlation is used:

$$\begin{aligned} c_{\mathrm{D}} &= 24.0/Re_{\mathrm{p}}(1.0 + 0.15 Re_{\mathrm{p}}^{0.687}), \quad Re_{\mathrm{p}} < 1000, \\ c_{\mathrm{D}} &= 0.44, \qquad\qquad\qquad\qquad\quad Re_{\mathrm{p}} \geqslant 1000. \end{aligned} \tag{15}$$

In order to calculate the particle motion Eq. (14) were integrated over the time step Δt and numerically solved along the trajectory. The time step was fixed with a value of 0.5 ms which is sufficiently small with respect to the particle response time and the inter-particle collision time. Periodic boundary conditions are applied for the particles according to the approach adopted in the LES, i.e. particles leaving the computational domain are re-injected on the opposite side with the same velocity.

In order to generate the instantaneous fluid velocity along the particle trajectory the so-called Langevin equation model is applied (Sommerfeld et al., 1993). In this approach, the fluid

fluctuation at the new particle position is correlated with that at the old position through a correlation function $R_{\mathrm{p},i}(\Delta t, \Delta r)$ in the following way:

$$\begin{aligned} u^f_{n+1} &= R_{\mathrm{p},u}(\Delta t, \Delta r) u^f_n + \sigma_u \sqrt{1 - R^2_{\mathrm{p},u}(\Delta t, \Delta r)}\,\xi, \\ v^f_{n+1} &= R_{\mathrm{p},v}(\Delta t, \Delta r) v^f_n + \sigma_v \sqrt{1 - R^2_{\mathrm{p},v}(\Delta t, \Delta r)}\,\zeta, \\ w^f_{n+1} &= R_{\mathrm{p},w}(\Delta t, \Delta r) w^f_n + \sigma_w \sqrt{1 - R^2_{\mathrm{p},w}(\Delta t, \Delta r)}\,\chi, \end{aligned} \tag{16}$$

where ξ, ζ, and χ are the Gaussian random numbers with a mean value of zero and a standard deviation of one. The first term on the right-hand side represents the correlated part and the second term the random contribution to the velocity fluctuation. The correlation function $R_{\mathrm{p},i}(\Delta t, \Delta r)$ is composed of a Lagrangian and Eulerian part, in order to account for the crossing trajectories effect in case gravity is considered:

$$R_{\mathrm{p},i}(\Delta t, \Delta r) = R_{\mathrm{L}}(\Delta t) \times R_{\mathrm{E},i}(\Delta r), \tag{17}$$

where the index i stands for the three components in the x, y, and z directions. For the Lagrangian velocity auto-correlation function an exponential form is selected

$$R_{\mathrm{L}}(\Delta t) = \exp\left(-\frac{\Delta t}{T_{\mathrm{L}}}\right). \tag{18}$$

The Lagrangian integral time scale, T_{L}, is determined from

$$T_{\mathrm{L}} = c_{\mathrm{T}} \frac{\sigma^2_{\mathrm{F}}}{\varepsilon} \quad \text{with } c_{\mathrm{T}} = 0.4, \tag{19}$$

where σ_{F} is the mean fluctuation of the fluid at the particle position, calculated from the turbulent kinetic energy by $\sigma^2_{\mathrm{F}} = 2/3\mathrm{k}$. In order to match the Lagrangian integral time scale of the LES, the dissipation rate ϵ was prescribed accordingly. The spatial correlation of the individual velocity components for two arbitrary points in space can be obtained from the Eulerian correlation tensor, $R_{\mathrm{E},ij}(\Delta r)$, by using the longitudinal and transverse correlation coefficients, $f(\Delta r)$ and $g(\Delta r)$ (Von Karman and Horwarth, 1938).

$$R_{\mathrm{E},ij}(\Delta r) = \{f(\Delta r) - g(\Delta r)\}\frac{r_i r_j}{r^2} + g(\Delta r)\delta_{ij}. \tag{20}$$

In the present calculations only the three main components (i.e. $R_{\mathrm{E},x}(\Delta r), R_{\mathrm{E},y}(\Delta r)$ and $R_{\mathrm{E},z}(\Delta r)$) are considered. The longitudinal and transverse correlation coefficients for homogeneous and isotropic turbulence are given by

$$\begin{aligned} f(\Delta r)_i &= \exp\left(-\frac{\Delta r}{L_{\mathrm{E},i}}\right), \\ g(\Delta r)_i &= \left(1 - \frac{\Delta r}{2L_{\mathrm{E},i}}\right)\exp\left(\frac{-\Delta r}{L_{\mathrm{E},i}}\right). \end{aligned} \tag{21}$$

The integral length scales for the three directions (i.e. streamwise component x and lateral components x and y) were determined from

$$L_{E,x} = 1.1\ T_L \sigma_F, \quad L_{E,y} = L_{E,z} = 0.5\ L_{E,x}. \tag{22}$$

The coefficient 1.1 was introduced in order to match the turbulent length scales of the LES.

4. Inter-particle collision model

The developed stochastic inter-particle collision model relies on the generation of fictitious collision partners and the calculation of the collision probability according to kinetic theory. The advantage of this model is that it does not require information on the location of the surrounding particles and hence it is also applicable if a sequential tracking of the particles is adopted, as usually done when applying the Euler/Lagrange approach to stationary flows. During each time step of the trajectory calculation of the considered particle a fictitious second particle is generated. The size and velocity of this fictitious particle are randomly sampled from local distribution functions.

The sampling of the fictitious particle size requires information on the local particle size distribution. Since in practical situations the particle size distribution may change throughout the flow field due to the different responses of different sized particles, the particle size distribution (i.e., the number frequency distribution) has to be sampled and stored for each control volume of the entire computational domain. This requires the size distribution to be resolved by a number of size classes. Typically about 20 size classes are sufficient. In many cases the particle size distribution may be represented by a log-normal distribution function which is characterised by a number mean diameter and a standard deviation. In such a case, only these two properties have to be stored for each control volume of the computational domain (Sommerfeld, 1995). Hence the size of the fictitious particle is randomly sampled from such a distribution function. In the present case where a binary mixture of particles with different densities is considered, a two-class density distribution is used where the probability for each class corresponds to the relative number concentrations. Therefore, the type of particle (i.e., heavy or light) is sampled from this two-class distribution.

The velocity components of the fictitious particle are composed of the local mean velocities and fluctuating components sampled from Gaussian velocity distributions with the local rms-value. In case, a particle size distribution is considered, also the particle size-velocity correlation has to be obtained for each control volume, i.e., the particle mean and rms velocities are sampled and stored for each size class.

In generating the fictitious particle fluctuating velocities the correlation with the velocity of the considered particle due to turbulence has to be respected. The degree to which the particle fluctuating velocities are correlated depends on their response to the turbulent fluctuations. The velocities of small particles will be strongly correlated, while those of very large particles are completely uncorrelated (i.e., kinetic theory limit). The response of particles to turbulent fluctuations is characterised in terms of the Stokes number, i.e., the ratio of the particle response time to the Lagrangian integral time scale of turbulence (Eq. (1)). The particle response time is determined from the calculations accounting for non-linear drag and the Lagrangian integral time scale is obtained from the turbulent dispersion model. In the developed collision model, the correlation of

the fluctuating velocity components of the fictitious particle $u'_{\mathrm{fict},i}$ with those of the real particle $u'_{\mathrm{real},i}$ is accounted for in the following way by using the turbulent Stokes number:

$$u'_{\mathrm{fict},i} = R(St)u'_{\mathrm{real},i} + \sigma_{\mathrm{p},i}\sqrt{1 - R(St)^2}\,\xi. \tag{23}$$

Here $\sigma_{\mathrm{p},i}$ is the local rms value of the particle velocity component i and ξ is a Gaussian random number with zero mean and a standard deviation of one. Hence, the sampled fluctuating velocity components are composed of a correlated and a random part. With increasing Stokes number the correlated term (first term in Eq. (23)) decreases and the random term increases accordingly. Comparing model calculations with large eddy simulations (which will be introduced below) the following dependence of the correlation function $R(St)$ on the Stokes number was found in the present study:

$$R(St) = \exp(-0.55 \times St^{0.4}). \tag{24}$$

The next step in the collision model is the determination of the probability for the occurrence of a collision between the considered and the fictitious particle within the time step. This probability is essentially the number of collisions within the time step which should be smaller than unity, if a proper time step constraint is applied. The collision probability is calculated as the product of the time step size Δt and the collision frequency given by kinetic theory:

$$P_{\mathrm{coll}} = f_{\mathrm{c}}\Delta t = \frac{\pi}{4}(D_{\mathrm{p},i} + D_{\mathrm{p},j})^2|\vec{u}_{\mathrm{p},i} - \vec{u}_{\mathrm{p},j}|n_{\mathrm{p}}\Delta t, \tag{25}$$

where $D_{\mathrm{p},i}$ and $D_{\mathrm{p},j}$ are the particle diameters, $|\vec{u}_{\mathrm{p},i} - \vec{u}_{\mathrm{p},j}|$ is the instantaneous relative velocity between the considered and the fictitious particle and n_{p} is the number of particles per unit volume in the respective control volume. At this point it should be noted that if a particle size distribution is considered, n_{p} should be the number concentration of all particle fractions, since the fictitious particle is sampled from the size distribution which already accounts for the probability of a particle being in a certain size interval. In order to decide whether a collision takes place, a random number RN from a uniform distribution in the interval [0,1] is generated. A collision is calculated when the random number becomes smaller than the collision probability, i.e. if

$$RN < P_{\mathrm{coll}}. \tag{26}$$

Since the considered particle or computational particle represents a number of real particles it is assumed that all these particles collide with the same number of fictitious particles. It is more complicated to determine the position of the fictitious particle relative to the considered particle. Since both particles move, any point on the surface of the particles is a possible point of contact. Moreover, the probability density for the point of impact is not the same for every point on the surface and strongly depends on the relative motion of the particles. Therefore, it is very difficult to model the collision in the co-ordinate system of the flow field in which both particles move. When the problem is however transferred into a co-ordinate system in which the fictitious particle is fixed, the collision calculation becomes much simpler. In this situation, the point of impact on the surface of the fictitious particle can only be located on the hemisphere facing the considered particle (Fig. 2). Now a collision cylinder is defined as the domain where the centre of the fictitious particle must be located if a collision takes place. It is physically obvious that the probability density of finding the centre of the fictitious particle at some point in the perpendicular cross-

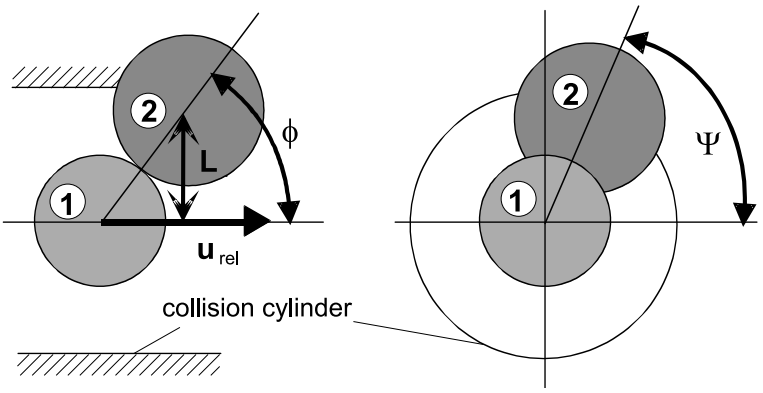

Fig. 2. Particle–particle collision configuration in a co-ordinate system with a stationary collision partner ②.

section of the cylinder is uniform. Note that this does not imply a uniform probability density for the points of impact on the particle surface. By generating two uniform random numbers XX and ZZ in the range [0, 1], the location of the collision point in the longitudinal section of the collision cylinder is defined by the lateral non-dimensional displacement, L (i.e. the lateral displacement is normalised by the sum of the two particle radii), and the angle ϕ (Fig. 2)

$$\begin{aligned} L &= \sqrt{XX^2 + ZZ^2} \quad \text{with } L < 1, \\ \phi &= \arcsin(L). \end{aligned} \tag{27}$$

In addition, the orientation of the collision plane in the cross-section of the collision cylinder (i.e. the angle Ψ) is randomly sampled from a uniform distribution in the range $[0 < \Psi < 2\pi]$.

The result of the sampling procedure for the impact point is given in Fig. 3. The distribution of the impact points in the cross-section of the collision cylinder is relatively uniform (Fig. 3(a)). However, the probability for the lateral displacement increases from zero at the axis of the collision cylinder to the maximum at the outer edge (Fig. 3(b)). The probability of the collision angle ϕ follows, as expected, a sinusoidal distribution function (Fig. 3(c)).

The relations for the calculation of the post-collision velocities of the considered particle in the co-ordinate system where the fictitious particle is stationary now reduce to the momentum equations for an oblique central collision. By solving the momentum equations in connection with Coulomb's law of friction and neglecting particle rotation, one obtains the following equations for the determination of the velocity components of the considered particle after rebound:

$$u'_{\mathrm{p1}} = u_{\mathrm{p1}}\left(1 - \frac{1+e}{1 + m_{\mathrm{p1}}/m_{\mathrm{p2}}}\right), \tag{28}$$

- non-sliding collision:

$$v'_{\mathrm{p1}} = v_{\mathrm{p1}}\left(1 - \frac{2/7}{1 + m_{\mathrm{p1}}/m_{\mathrm{p2}}}\right), \tag{29}$$

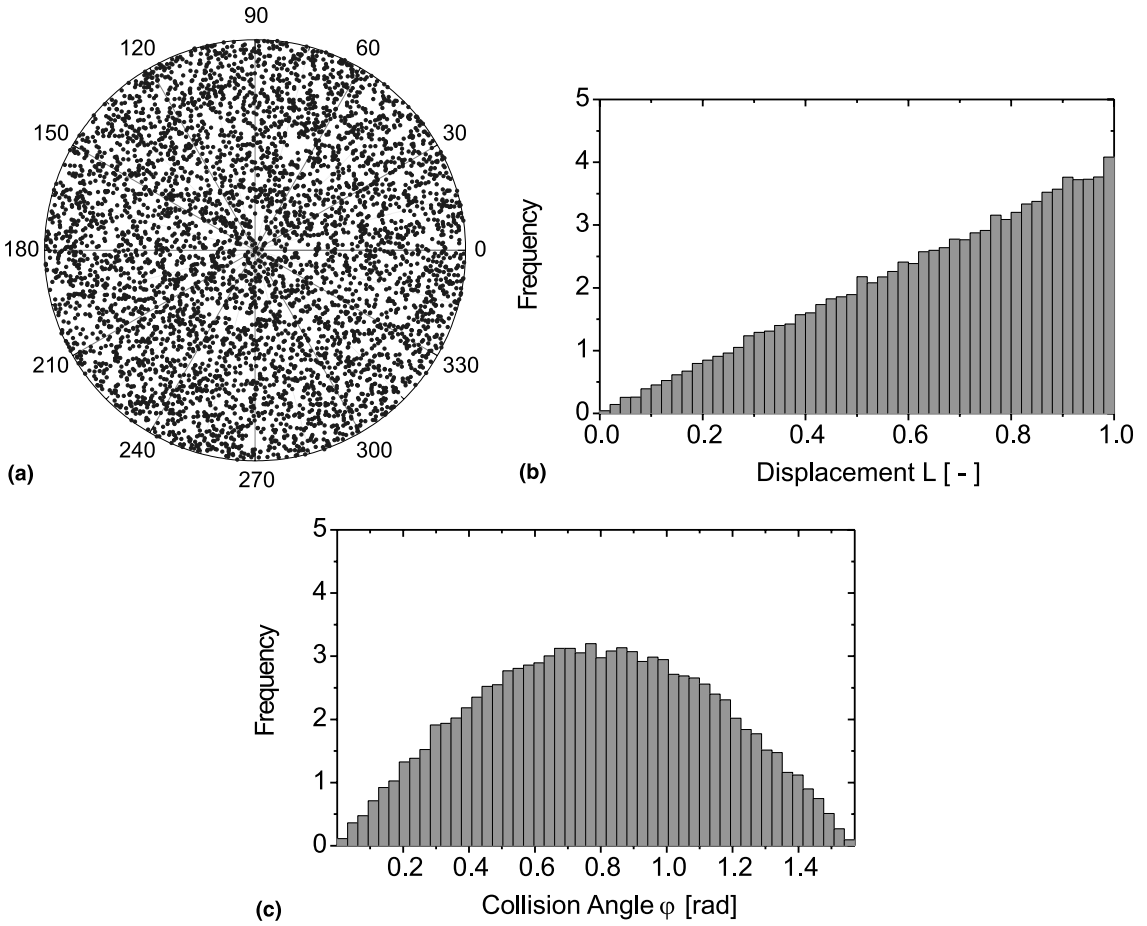

Fig. 3. Probability distributions of sampled location of the impact point: (a) in the cross-section of the collision cylinder, (b) lateral displacement L, (c) collision angle ϕ.

- sliding collision:

$$v'_{p1} = v_{p1}\left(1 - \mu(1+e)\frac{u_{p1}}{v_{p1}}\frac{1}{1+m_{p1}/m_{p2}}\right), \tag{30}$$

- condition for a non-sliding collision:

$$\frac{u_{p1}}{v_{p1}} < \frac{7}{2}\mu(1+e). \tag{31}$$

Here e is the coefficient of restitution, μ is the coefficient of friction, and m_{p1} and m_{p2} are the masses of the considered and the fictitious particle, respectively. Finally, the velocities of the considered particle are re-transformed in the original co-ordinate system.

An essential requirement for the collision model is however, that for each control volume the particle size and the velocity distribution functions have to be sampled and stored. The local

distribution functions of the particle phase properties are updated after each Lagrangian calculation through an iterative procedure until these properties approach steady-state values. Since in the first iteration no particle phase properties are available yet, the particle collision calculation begins with the second Lagrangian calculation. When the effect of the particles on the fluid flow is accounted for, this procedure is combined with the two-way coupling iteration procedure (Kohnen et al., 1994).

5. Homogeneous isotropic turbulence

The first test case considered to validate the developed stochastic Lagrangian inter-particle collision model is a homogeneous isotropic turbulence field in a cube with periodic boundary conditions where data obtained by LES are available (Lavieville et al., 1995). The turbulence characteristics and the particle properties are summarised in Table 1. The collision detection algorithm adopted in the LES required to consider rather large particles (i.e. $D_p = 656$ μm). In order to have particle response times which are in the order of the integral time scale of turbulence, the particle material density was selected to be relatively small (Table 1). The resulting turbulent Stokes numbers (Eq. (1)) are between about 0.8 and 6.0. However, the model calculations were also performed for a wider range of Stokes numbers as shown below. Since for this case no gravity is considered the particle motion is solely controlled by turbulence and collisions. The collisions are assumed to be fully elastic (i.e. $e = 1.0, \mu = 0.0$).

Additionally, Table 1 includes the value for the viscous dissipation estimated from the LES based on the balance of the turbulent kinetic energy. This also gives an estimate of the Kolmogorov time scale which is about 15 times smaller than the integral time scale of turbulence. Since these values may be only very approximately estimated from the LES a reliable determination of the collision rate introduced by Saffman and Turner (1956) for particles following the fluid is unfortunately not possible in the limit of $St \to 0$.

The model calculations were performed for 2000 particles each being tracked for 3 s. The starting location of the particles was randomly selected within the entire computational domain of

Table 1
Turbulence characteristics and particle phase properties for the large eddy simulations

Gas phase rms velocity	0.3 m/s
Gas density	1.17 kg/m^3
Dynamic viscosity	17.2×10^{-6} kg/m s
Viscous dissipation (estimated)	6.17 m^2/s^3
Lagrangian integral time scale	23 ms
Kolmogorov time scale (estimated)	1.544 ms
Eulerian integral time scale	26 ms
Longitudinal Eulerian length scale	7.25 mm
Lateral Eulerian length scale	3.71 mm
Particle diameter	0.656 mm
Particle density	25, 50, 100, 200 kg/m^3
Turbulent Stokes number	0.79, 1.5, 2.9, and 5.7
Volume fraction	0.005–0.05

0.2 m × 0.2 m × 0.2 m. The initial particle velocity components were sampled from a normal distribution function with a mean velocity of zero and an rms value which was between 20% and 100% of that of the gas phase, depending on the particle Stokes number. Particles leaving the computational domain at one face of the cube were re-injected on the opposite side with the same velocity. This procedure was continued until the total tracking time of 3 s was reached. Then the next particle trajectory was started.

As expected, the energy of the particles' fluctuating motion decreases with increasing Stokes number, since the particles become less responsive to the turbulent fluctuations (Fig. 4). For very small Stokes numbers the ratio k_p/k approaches unity, whereas for very large Stokes numbers the ratio approaches zero. Both the model calculations and the simulations follow the same trend, indicating that the particle-turbulence interaction is modelled properly (Fig. 4). The collisions between the particles have no strong influence on the particles fluctuating motion, i.e. the results for the different volume fractions are only slightly different. The effect of inter-particle collisions on the fluctuating motion of the particles becomes more obvious when considering the Lagrangian velocity correlation of the particles. This correlation function was calculated along the particle trajectories for different time intervals from a starting time which allowed the particles to adjust to the flow after being injected into the flow domain. Hence, the Lagrangian correlation function was sampled by applying the following equation:

$$R_{\mathrm{Lp},j}(t_0 + i\Delta t) = \frac{1}{N_k} \sum \frac{u_{\mathrm{p},j,k}(t_0) \times u_{\mathrm{p},j,k}(t_0 + i\Delta t)}{\sqrt{\overline{u^2_{\mathrm{p},j}(t_0)} \times \overline{u^2_{\mathrm{p},j}(t_0 + i\Delta t)}}}, \tag{32}$$

where the index j stands for the three velocity components, N_k is the number of particle trajectories considered (typically 2000 for sampling the correlation function) and $i\Delta t$ is the time separation from the initial time with i being the number of equidistant time steps. In Fig. 5 Lagrangian correlation functions for different volume fractions (i.e. with inter-particle collisions) are compared with those obtained without inter-particle collisions. It is obvious that due to the

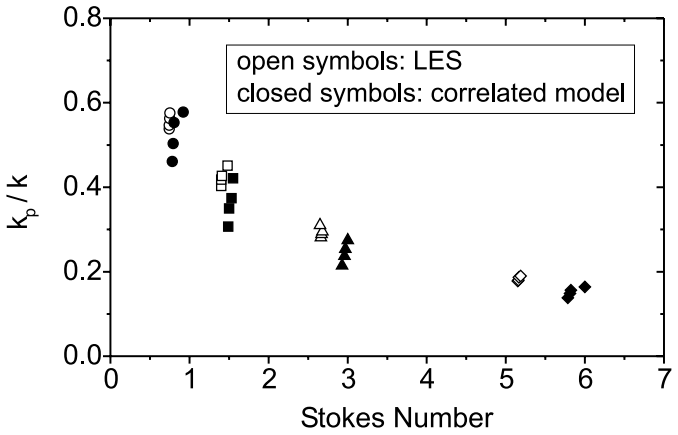

Fig. 4. Kinetic energy of the particle fluctuating motion as a function of the Stokes number (symbols of one kind indicate the results for the different volume fractions).

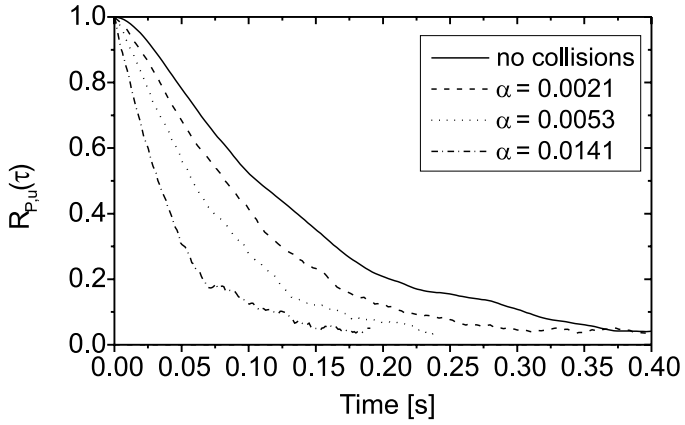

Fig. 5. Lagrangian correlation functions of the particles obtained from the model calculations for different volume fractions ($\rho_p = 200$ kg/m^3, $St = 5.7$).

randomness of inter-particle collisions, the fluctuation velocity of the particles becomes more and more uncorrelated with increasing volume fraction and hence increasing collision frequency.

By integrating the correlation function also the Lagrangian integral time scale of the particles fluctuating motion may be obtained and compared with the LES data. This is done in Fig. 6 for two particle densities (i.e. Stokes numbers of 1.5 and 5.7) by normalising the particles Lagrangian time scale with the Lagrangian time scale of the fluid viewed by the particles. The agreement between LES and model calculations is reasonably good also for this value. As a result of the inertia of the heavier particles their Lagrangian integral time scale decays faster due to collisions than that of the lighter particles with increasing volume fraction.

An important feature of the developed stochastic collision model is the consideration of the correlated motion of colliding particles. This effect is pronounced when the particle response time is in the order of the integral time scale of turbulence or even lower. The relative velocity

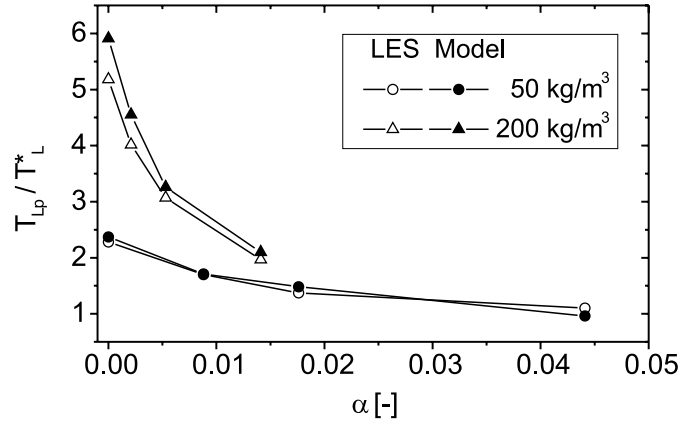

Fig. 6. Lagrangian integral time scale as a function of the volume fraction for light and heavy particles, comparison of LES data with model calculations ($\rho_p = 50$ kg/m^3, $St = 1.5$, $\rho_p = 200$ kg/m^3, $St = 5.7$).

distribution function (PDF) for particles with a Stokes number of 0.79, shown in Fig. 7(a), reveals the importance of accounting for this correlation. Please note that the modulus of the relative velocity includes all three velocity components. If the fluctuating velocity of the fictitious particle is not correlated with that of the considered particle a rather wide velocity distribution with a mean value of 0.48 m/s is obtained. The correlated model on the contrary gives a more narrow relative velocity distribution with a mean value reduced to 0.33 m/s. The comparison of the model calculations with the large eddy simulations shows a rather good agreement if the degree of correlation is modelled appropriately by specification of the model constants in the correlation function (Eq. (24)).

Also the distribution function of the angle between the trajectories of colliding particles is considerably shifted towards smaller angles when accounting for the correlation of velocities in the model (Fig. 7(b)). The calculated angle probability density function (PDF) agrees well with the LES result and a mean value of 1.07 rad is calculated. Without the velocity correlation a larger mean value of 1.76 rad is obtained.

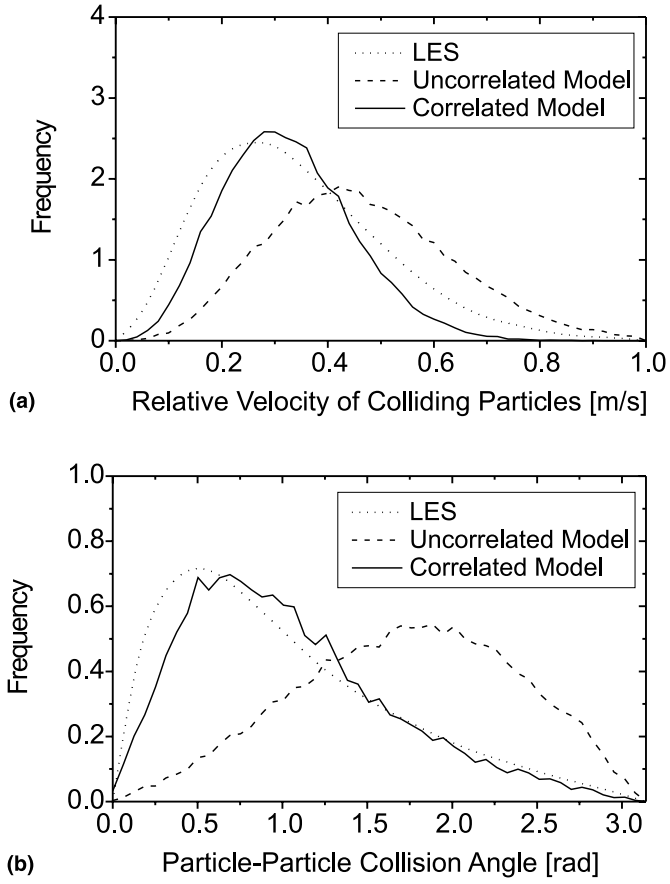

Fig. 7. Distribution of the mean relative velocity modulus between colliding particles, (a) and the particle–particle collision angle (b), comparison of the stochastic model with large eddy simulations ($\rho_p = 25$ kg/m^3, $St = 0.79$, $\alpha = 0.0352$).

When considering heavier particles (i.e. $\rho_p = 200\ \mathrm{kg/m^3}, St = 5.8$) the relative velocity is slightly underestimated by the correlated model in comparison to the LES results but the particle–particle collision angle matches fairly well (Fig. 8).

From the above results it is obvious that the correlated motion of particles in turbulent flows has the following consequences:

- reduction in the mean relative velocity,
- reduction in the standard deviation of the relative velocity distribution and
- reduction of the particle–particle collision angle.

In the following these effects will be demonstrated for a wider range of Stokes numbers than those considered in the computationally expensive LES. The effect of Stokes number on the mean relative velocity of colliding particles is illustrated in Fig. 9 for model calculations with and without correlation. As a result of the higher agitation of small particles by turbulence the uncorrelated model considerably overpredicts the mean relative velocity. The correlated model predicts an increase of the mean relative velocity with decreasing Stokes number up to a Stokes

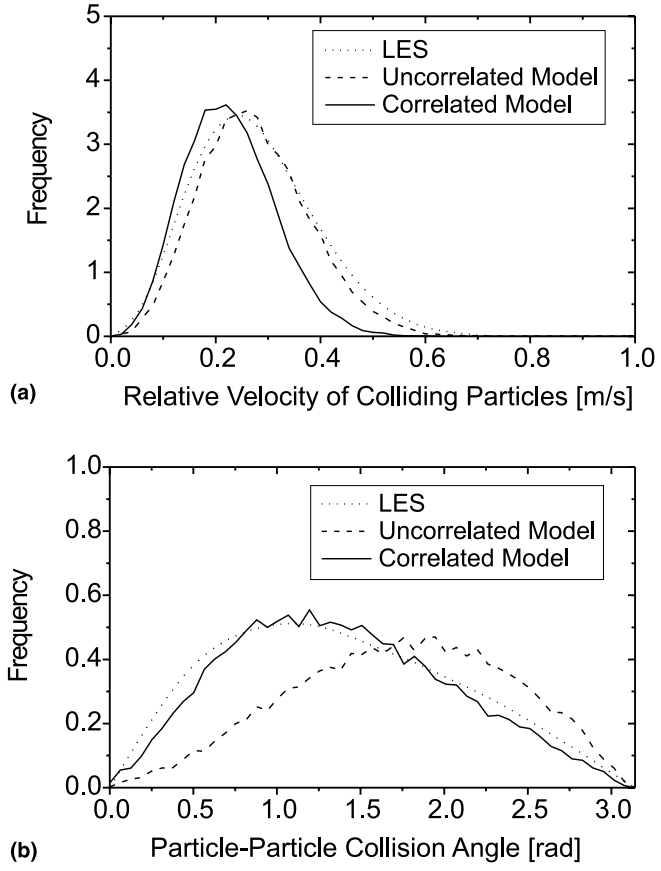

Fig. 8. Distribution of the mean relative velocity modulus between colliding particles (a) and the particle–particle collision angle (b), comparison of the stochastic model with large eddy simulations ($\rho_p = 200\ \mathrm{kg/m^3}$, $St = 5.8$, $\alpha = 0.0141$).

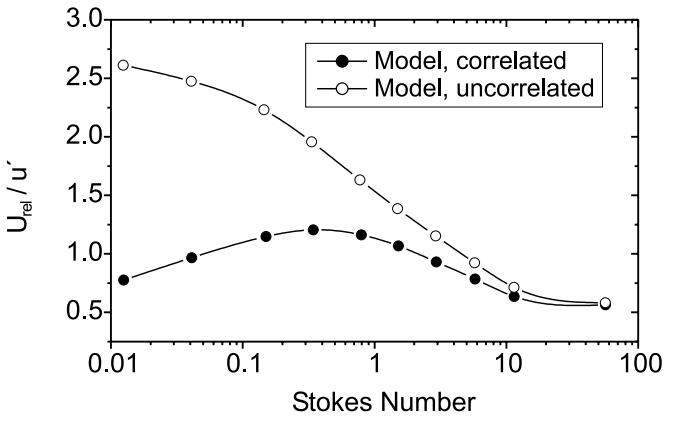

Fig. 9. Modulus of the mean relative velocity of colliding particles as a function of Stokes number, comparison of uncorrelated and correlated model ($\alpha = 0.0176$).

number of about 0.4. With further reducing the particle Stokes number, the velocity of colliding particles becomes more and more correlated and hence a decrease in the mean relative velocity is observed. For small particles a limiting value is approached corresponding to particles completely following the turbulent fluctuations. By not accounting for the velocity correlation for light particles, the mean relative velocity and hence the collision frequency are completely overpredicted. For heavy particles the same mean relative velocity is obtained as for the kinetic theory approach which one would of course expect.

A similar behaviour is observed for the mean square value of the relative velocity distribution (Fig. 10). The uncorrelated model (i.e. kinetic theory) gives a continuous broadening of the relative velocity distribution with decreasing Stokes number, while the correlated model predicts considerably smaller values for Stokes numbers below about 10. For comparison also the fitting proposed by Williams and Crane (1983) is included in Fig. 10. Their correlation (see Eq. (5)) shows the same behaviour as the proposed correlated model, but with a maximum in the mean

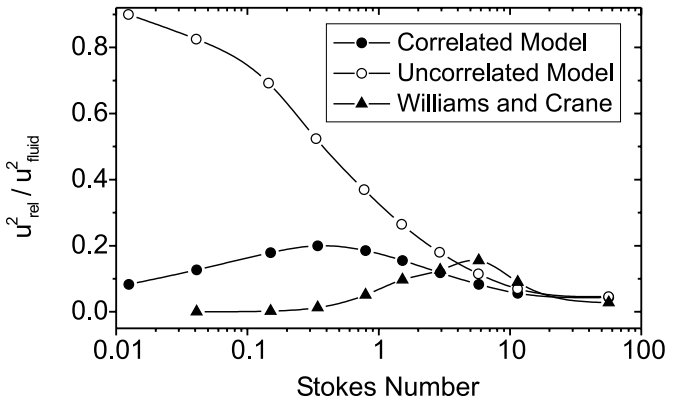

Fig. 10. Mean square value of the absolute relative velocity of colliding particles, comparison of uncorrelated and correlated models ($\alpha = 0.0176$) and with the correlation proposed by Williams and Crane (1983).

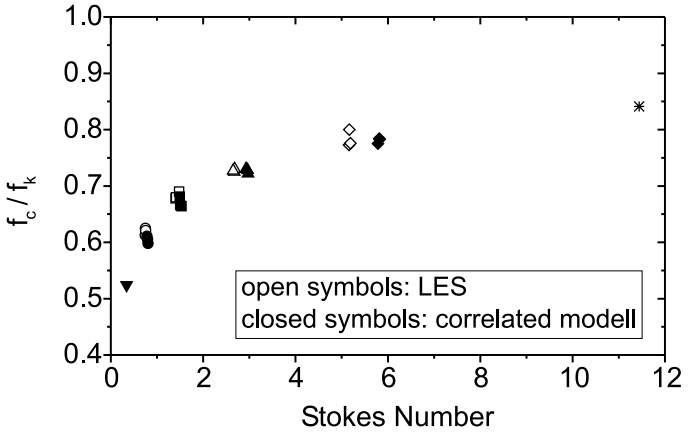

Fig. 11. Dependence of the ratio of simulated collision frequency to the collision frequency obtained from the kinetic theory limit on the particle Stokes number (symbols of one kind indicate the results for the different volume fractions, see Table 1).

square value located near a Stokes number of 6. Moreover, their values in this region are slightly above the result obtained from kinetic theory which reveals some deficiencies of their fitting. Since solid particles in air are considered in the present study, the correlation proposed by Williams and Crane (1983) is identical with that provided by Kruis and Kusters (1997).

As a result of the reduction of the mean relative velocity due to the correlation effect, also the average collision frequency will be reduced. This effect may be illustrated by comparing the simulated average collision frequency with that resulting from the kinetic theory limit, which corresponds to the average collision frequency obtained without correlation. In Fig. 11 the ratio of the calculated collision frequency to that predicted by kinetic theory is plotted versus Stokes number. For very large Stokes numbers the frequency ratio approaches unity. With decreasing Stokes number the frequency ratio is continuously reduced due to the increasing degree of correlated motion of colliding particles. The predicted increase of the frequency ratio with Stokes number is in very good agreement with the LES data.

Fig. 12 shows the collision frequency obtained from the model calculations for a wider range of Stokes numbers. As expected from the mean relative velocity, the uncorrelated model predicts a continuous increase of the collision frequency with decreasing Stokes number. The correlated model however predicts a maximum in the collision frequency for a Stokes number of about 0.4. For smaller Stokes numbers a decrease of the collision frequency is found and in the limit of particles completely following the turbulent fluctuations (i.e. $St \rightarrow 0$) will be approached. The predicted shape of both curves is very similar to the result of Sundaram and Collins (1997) obtained by DNS for different turbulence properties.

6. Binary mixture of particles

The second test case for validating the stochastic inter-particle collision model was again an isotropic homogeneous turbulence. However, now a binary mixture of particles (fractions A and

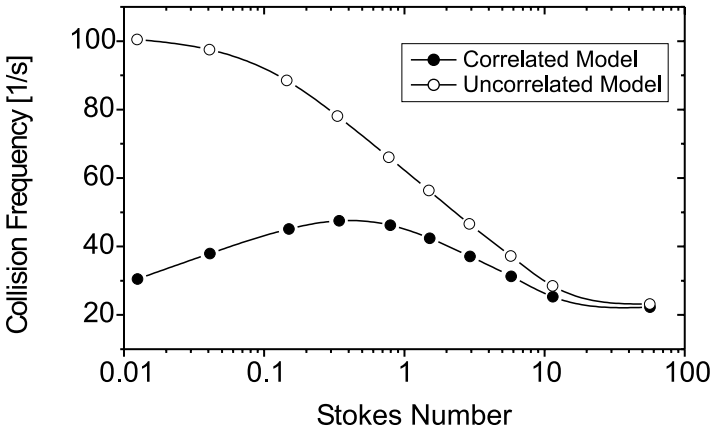

Fig. 12. Dependence of the ratio of simulated collision frequency to the collision frequency obtained from the kinetic theory limit on the particle Stokes number ($\alpha = 0.0176$).

B) is considered. In the LES of Gourdel et al. (1998) the same turbulence properties were used as in the previous case (see Table 1). The particle size was 650 μm and two classes of particles (i.e. with different response times) were generated by using different densities (i.e. $\rho_A = 117.5$ kg/m^3 and $\rho_B = 235$ kg/m^3). The volume fraction of class A particles was fixed with 1.3×10^{-2} and that of class B particles was varied between 6.5×10^{-4} and 4×10^{-2}. Again completely elastic collisions were considered (i.e. $e = 1.0, \mu = 0$).

The first series of calculations was performed for a granular medium without particle-fluid interaction and under zero-gravity conditions in a cube with 0.2 m × 0.2 m × 0.2 m. This implies that the particle motion is solely governed by inter-particle collisions and the initial fluctuation of the particles upon injection into the computational domain. The particle injection and tracking procedure was identical to that for the case of the isotropic homogeneous turbulence. The initial particle velocity components upon injection were sampled from a normal distribution function with a mean velocity of zero and a fixed rms value of 0.29 m/s for all cases considered.

For validating the model calculations the velocity distributions of one component for both particle fractions were compared with the results from the LES. From Fig. 13 it is obvious that the model results are in excellent agreement with the simulations. In the following the kinetic energy of the particles fluctuating motion is used to characterise the effect of inter-particle collisions (Fig. 14). As expected the kinetic energy of fluctuation is higher for the lighter particles (class A) than for the heavier particles (class B). With increasing total number density (i.e. in this case the number density of fraction A is constant and the number density of fraction B is increasing) the energy of particle fluctuation is increasing for both fractions due to the increase in total collision frequency. The model calculations are in good agreement with the LES-data. Only for large concentrations of fraction B, a slight overprediction of the fluctuations of both fractions is observed.

The calculated collision frequencies between particles of fraction A (f_{AA}) and between both fractions (f_{AB}) as a function of the volume fraction of class B particles are compared in Fig. 15 with the results of the LES. The collision frequency f_{AA} slightly increases with the volume fraction α_B, since the fluctuating intensity of fraction A particles is increasing (see Fig. 14). With increasing

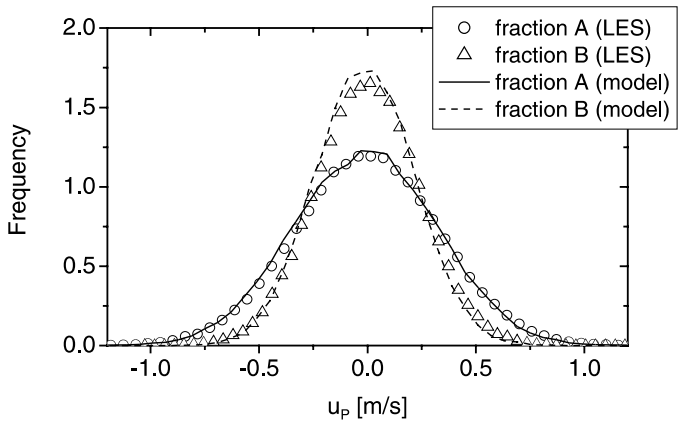

Fig. 13. Particle velocity distributions for both fractions, comparison of model calculations and LES results ($\alpha_A = 1.3 \times 10^{-2}$ and $\alpha_B = 5.0 \times 10^{-4}$).

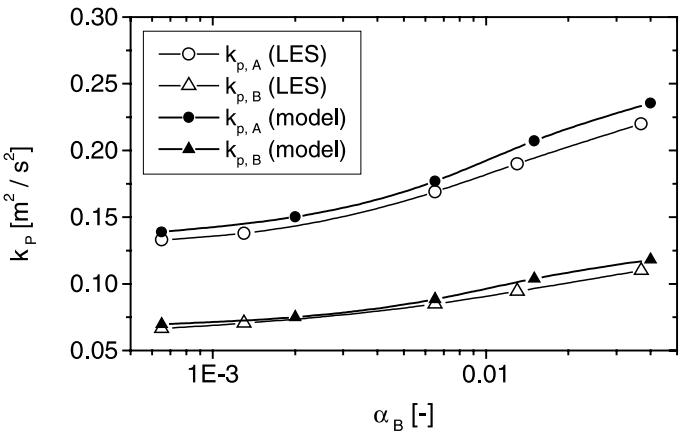

Fig. 14. Kinetic energy of particle fluctuating motion for fractions A and B, comparison of model calculations with LES data for a granular medium.

the fraction of B-particles the collision frequency f_{AB} increases linearly as expected. Similarly, the collision frequency between fraction B particles increases linearly with the volume fraction of B-particles (Fig. 16). Since the number concentration of A-particles is constant, the collision frequency f_{BA} only is slightly increasing with α_B, again as a result of the increasing fluctuation intensity of both fractions. All these effects are very well captured by the model calculations and the agreement with the LES is very good (Figs. 15 and 16).

In the second case, a binary mixture settling under the action of gravity (i.e. $g_x = 49.05\ \mathrm{m/s^2}$) in a cube with homogeneous isotropic turbulence is considered. Since for this situation the particles are settling through the computational domain, the inlet and boundary conditions are different from those in the previous case. The particles are injected in the direction of gravity randomly distributed over the inlet face of the cube. The initial particle velocity component in the direction of gravity for both particle classes was sampled from a normal distribution function with a mean

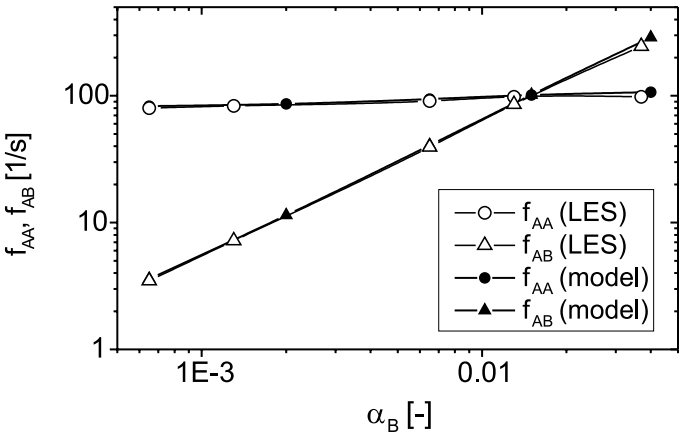

Fig. 15. Collision frequencies for fraction A and between fractions A and B, comparison of model calculations with LES data for a granular medium.

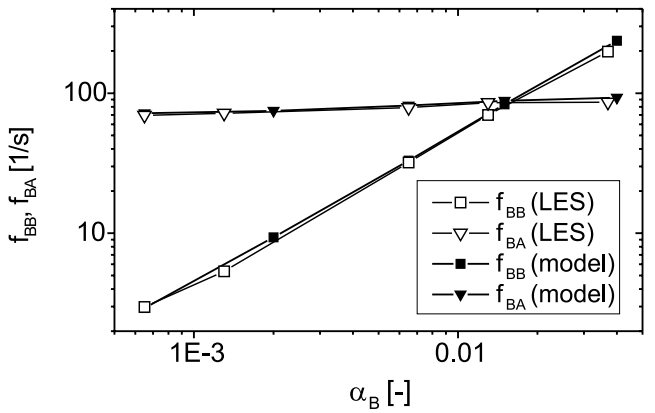

Fig. 16. Collision frequencies for fraction B and between fractions B and A, comparison of model calculations with LES data for a granular medium.

value close to the terminal velocity and an rms value which was between 20% and 100% of that of the gas phase, depending on the particle Stokes number. For the lateral velocity components particle mean velocities of zero and rms values corresponding to the streamwise component were specified. Each (computational) particle is again tracked for 3 s with a fixed time step of 0.5 ms. Particles leaving the computational domain at one face of the cube are re-injected at the opposite during this time period. In order to obtain a steady state situation at the end of the computation, the particle inlet velocities (mean velocities and rms values) are updated during the iteration process. This implies that after tracking 2000 particles, each for 3 s, new velocities of the particles are obtained and used as inlet condition for the next iteration step. For the considered cases, 20 iterations were found to be sufficient to approach a steady state situation.

The collisions between particles in this test case are mainly determined by the mean drift between the two particle fractions as a result of their different terminal velocities. In addition

collisions are induced by the fluctuating motion of the particles which is partly caused by turbulence. Hence, the collisions between the two particle fractions cause a momentum transfer between the two fractions, whereby the mean velocity (i.e. in the direction of gravity) of the light particles (fraction A) becomes larger than their terminal velocity and for the heavy particles the settling is hindered by collisions with the light particles (Fig. 17). At low volume fractions of class B particles, the heavy particles are strongly hindered by the light ones and hence the heavy particle mean velocity is about 19% smaller than their terminal velocity. With increasing volume fraction of class B, the heavy particles drag the light particles and their mean velocity increases, while the mean velocity of the heavy particles also increases and approaches the expected terminal velocity. These effects are well reproduced in the model calculations and the agreement with the LES-results is reasonably good.

Some larger differences between LES and model results are found for the kinetic energy of the particles (Fig. 18). Below a volume fraction of $\alpha_B = 4 \times 10^{-3}$ the fluctuating energy is underestimated by the model, whereas above this value an overprediction is found. One reason may be the slight overprediction of the mean velocity of the lighter particles (Fig. 17). However, the increase of the kinetic energy of the light particles (fraction A) with the volume fraction α_B is also captured by the model. The fluctuating energy of the heavy particles on the other hand is not changing largely with their volume fraction. It should be also emphasised that the particles fluctuating motion is considerably damped by the interaction with the flow. This is obvious by comparing the result in Fig. 18 with that for the granular medium (Fig. 14).

Considering the collision frequencies for this case (Fig. 19), it is obvious that f_{AA} is considerably smaller than for the granular medium (Fig. 15), which is caused by the particle-flow interaction. With increasing concentration of fraction B the collision frequency of fraction A (f_{AA}) increases at a higher rate compared to the result in Fig. 15 due to a stronger increase of the fluctuating motion of fraction A (see Fig. 18). The collision frequencies between fractions A and B are about the same than for the granular medium. This indicates that the reduction of collision frequency due to particle-flow interaction is balanced by the mean relative drift between both fractions. The

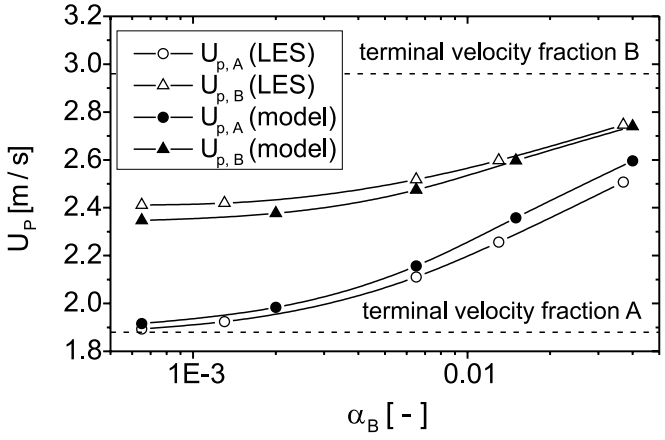

Fig. 17. Mean particle velocities for fractions A and B, comparison of model calculations with LES data for a binary mixture settling under gravity.

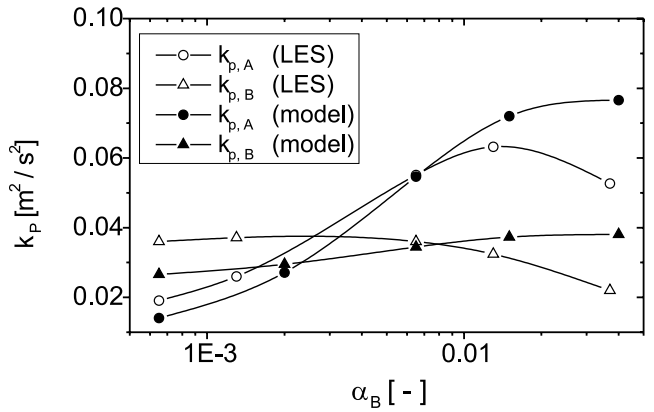

Fig. 18. Kinetic energy of the particles fluctuating motion for fractions A and B, comparison of model calculations with LES data for a binary mixture settling under gravity.

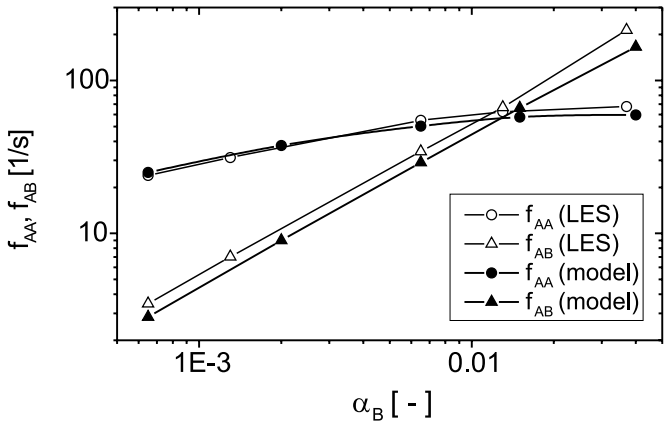

Fig. 19. Collision frequencies for fraction A and between fractions A and B, comparison of model calculations with LES data for a binary mixture settling under gravity.

comparison with the LES data shows a slight underprediction of the collision frequency f_{AB}, which is associated mainly with the underprediction of the mean drift between the two particle fractions (see Fig. 17).

In the calculations introduced so far, the collision process was assumed to be perfectly elastic. In practical situations however an inter-particle collision is inelastic and associated with friction between the particles. In order to analyse these effects, additionally calculations for different restitution and friction coefficients were performed for the binary mixture of particles settling under gravity in a homogeneous isotropic turbulence. Both the friction coefficient and the restitution ratio considerably altered the fluctuating motion of the particles. As a result of the energy dissipation through inter-particle collisions the kinetic energy of the particles fluctuation is considerably damped for both fractions (Fig. 20). However, the damping is more pronounced for the light particles (Fig. 20(a)) whereby the fluctuating energies of both fractions approach each other

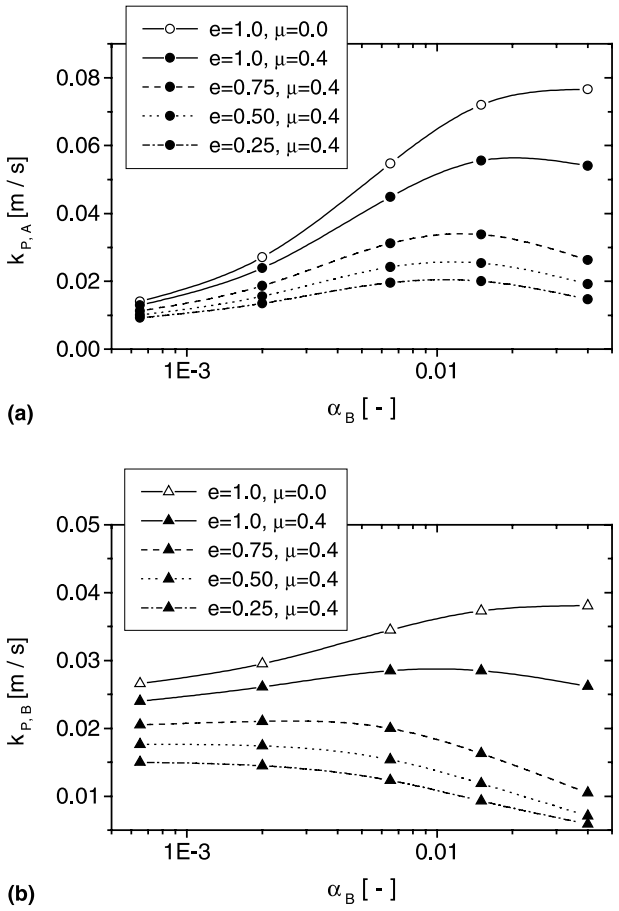

Fig. 20. Influence of restitution coefficient and friction on the kinetic energy of the particles fluctuating motion for fractions A and B (binary mixture settling in homogeneous isotropic turbulence).

with decreasing restitution ratio (i.e. with increasing momentum loss). In addition the damping effect becomes more pronounced with increasing overall volume fraction of particles since the number of inter-particle collisions is also linearly increasing with particle concentration (Fig. 20).

The reduction of the particle mean fluctuating velocities with decreasing restitution coefficient also has a considerable effect on the collision frequency. Since the collisions between particles of fraction A (f_{AA}) and B (f_{BB}) are determined by the fluctuating motion of the particles, both collision frequencies are reduced (Fig. 21(a) and (b)) by considering friction and/or inelastic collisions. With decreasing restitution coefficient a continuous reduction is observed. The collisions between the two particle fractions (i.e. f_{AB} and f_{BA}) are not only caused by their fluctuating motion, but mainly by the mean drift between them. The mean drift velocity between the two fractions on the other hand is the result of the momentum transfer induced by inter-particle collisions. Since inelastic collisions are associated with a momentum loss the available momentum to be transferred between the two fractions is reduced. Hence, the mean drift between the heavy and light particles is increasing with decreasing restitution coefficient (Fig. 22). For the case with

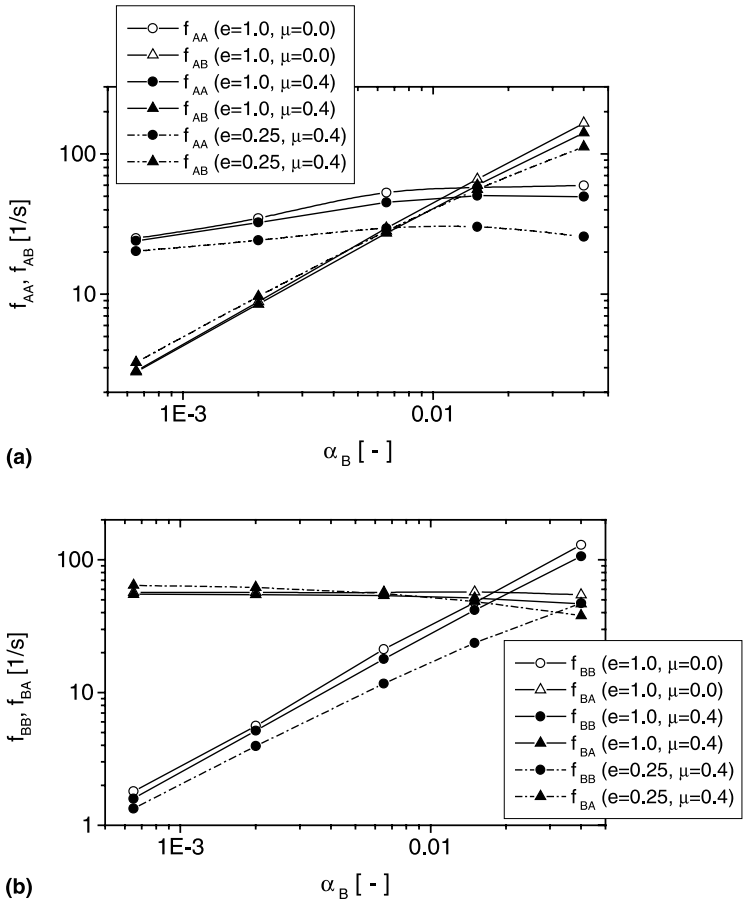

Fig. 21. Influence of restitution coefficient and friction on the collision frequencies f_{AA}, f_{AB}, f_{BB}, and f_{BA} (binary mixture settling in homogeneous isotropic turbulence).

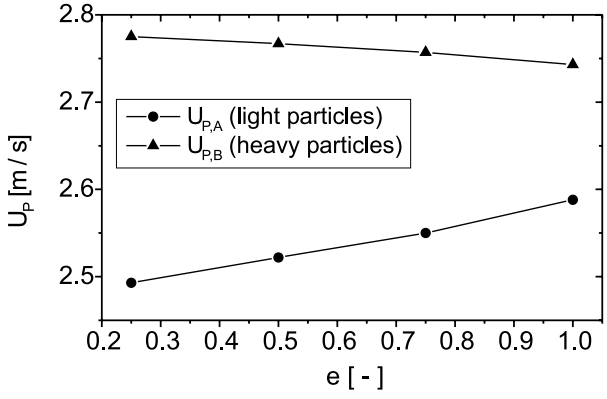

Fig. 22. Influence of restitution coefficient on the mean particle velocities for fractions A and B (binary mixture settling in homogeneous isotropic turbulence, $\alpha_B = 0.04, \mu = 0.4$).

the highest volume fraction (i.e. $\alpha_B = 4.0 \times 10^{-2}$) the heavy particle settling velocity is increasing and the light particle settling velocity is again reduced or remains constant for the smallest volume fraction $\alpha_B = 6.5 \times 10^{-3}$, both with decreasing restitution ratio. Therefore, the collision frequencies f_{AB} and f_{BA} are influenced by two effects:

- The reduction of the mean fluctuating velocity should reduce these collision frequencies, especially for larger α_B.
- The increase of the mean drift should increase the collision frequencies, especially at lower α_B.

These effects explain the modification of the collision frequencies f_{AB} and f_{BA} shown in Fig. 21. For low α_B (i.e. up to about $\alpha_B = 5.0 \times 10^{-3}$) the consideration of inelastic collisions results in a slight increase of the collision frequencies between the two fractions, whereas, at higher values of α_B a more pronounced decrease is observed.

7. Conclusions

It has been demonstrated that the developed stochastic inter-particle collision model predicts the correct particle phase properties and collision frequencies for the behaviour of monodisperse particles in a homogeneous isotropic turbulence field if the correlation of the velocities of colliding particles is accounted for properly. The model calculations for the dependence of the collision frequency on the turbulent particle Stokes number for a given volume fraction of particles show a maximum in the collision frequency for Stokes numbers of about 0.4. With decreasing Stokes number the collision frequency is reduced due to the increasing velocity correlation of colliding particles and a limiting value is approached for particles following the turbulence. With increasing Stokes number the collision frequency reduces and approaches the kinetic theory limit. Model calculations without considering the correlated particle motion in a homogeneous turbulence field yield a considerable overprediction of the collision frequencies for particle Stokes numbers below about 10. For the smallest Stokes numbers considered the difference is about one order of magnitude.

Also the collision frequencies of a granular medium (i.e. without particle-flow interaction) consisting of two fractions of particles and the associated fluctuating velocities could be correctly predicted by the model. In the case of a binary mixture settling under the action of gravity in a homogeneous isotropic turbulence, the momentum transfer between the two fractions due to collisions becomes important in the prediction of the terminal velocities. The effect that the light particles hinder the settling of the heavy particles if their volume fraction is low and that a high volume fraction of heavy particles results in a dragging of the light particles is properly predicted by the model and a good agreement with the LES data is obtained.

The analysis of the effect of inelastic and frictional collisions for the binary mixture settling under gravity revealed a considerable damping of the fluctuating velocities of both particle fractions with decreasing coefficient of restitution and increasing friction coefficient. This demonstrates the great importance of accounting for inelastic collisions when a prediction of practical gas-particle systems is anticipated. Moreover, detailed data are required of the restitution and friction coefficients for inter-particle collisions.

The introduced stochastic inter-particle collision model for the Euler/Lagrange approach is very economic with regard to computer time, since it does not require to search for possible collision partners in the vicinity of the considered particle.

Since the present model is limited to inertial particles with respect to the dissipation scale of turbulence, further studies are required to extend the range of validity to very small particles. Moreover, the present model is valid only for a 100% collision efficiency, namely for cases were the particle size is not too different. The model has been already extended to allow the consideration of the collision of small and large particles on the basis of a theoretically evaluated impact efficiency. This extension is especially important for agglomeration processes.

Acknowledgements

The financial support for the present studies by the Deutsche Forschungsgemeinschaft (DFG) under contract So 204/12-1 and 2 is gratefully acknowledged. Furthermore, the author would like to thank Prof. O. Simonin for providing the LES data and many helpful discussions.

References

Abrahamson, J., 1975. Collision rates of small particles in a vigorously turbulent fluid. Chem. Eng. Sci. 30, 1371–1379.

Burmester De Bessa Ribas, R., Lourenco, L., Riethmuller, M.L., 1980. A kinetic model for a gas-particle flow. Pneumotransport 5. In: Proceedings of the Fifth International Conference on the Pneumatic Transport of Solids in Pipes, Paper B2, pp. 99–112.

Crowe, C.T., 1981. On the relative importance of particle–particle collisions in gas-particle flows. In: Proceedings of the Conference on Gas Borne Particles, Paper C78/81, pp. 135–137.

Gourdel, C., Simonin, O., Brunier, E., 1998. Modelling and simulation of gas–solid turbulent flows with a binary mixture of particles. In: Third International Conference on Multiphase Flow, Lyon, France, June 1998.

Gourdel, C., Simonin, O., Brunier, E., 1999. Two-Maxwellian equilibrium distribution function for the modelling of a binary mixture of particles. In: Werther, J. (Ed.), Circulating Fluidised Bed Technology VI, Proceedings of the 6th International Conference on Circulating Fluidised Beds, DECHEMA, Frankfurt (Main) Germany, pp. 205–210.

Ho, C.A., Sommerfeld, M., 2001. Agglomeration of particles in turbulent flow: A stochastic Lagrangian model. International Congress for Particle Technology, PARTEC 2001, Paper No. 048.

Kohnen, G., Rüger, M., Sommerfeld, M., 1994. Convergence behaviour for numerical calculations by the Euler/Lagrange method for strongly coupled phases. In: Crowe et al. (Eds.), Numerical Methods in Multiphase Flows, vol. 185. 1994, ASME FED- pp. 191–202.

Kruis, F.E., Kusters, K.A., 1997. The collision rate of particles in turbulent flow. Chem. Eng. Comm. 158, 201–230.

Lavieville, J., Deutsch, E., Simonin, O., 1995. Large eddy simulation of interactions between colliding particles and a homogeneous isotropic turbulence field. In: Stock et al. (Eds.), Gas-Particle Flows, FED-vol. 228. ASME, pp. 359–369.

Lourenco, L., Riethmuller, M.L., Essers, J.-A., 1983. The kinetic model for particle flow and its numerical implementation. In: Proceedings of the International Conference on Physical Modelling of Multi-Phase Flows, Paper C4, pp. 501–525.

Mei, R., Hu, K.C., 1999. On the collision rate of small particles in turbulent flows. J. Fluid Mech. 391, 67–89.

Oesterle, B., Petitjean, A., 1993. Simulation of particle-to-particle interactions in gas–solid flows. Int. J. Multiphase Flow 19, 199–211.

Pearson, H.J., Valioulis, I.A., List, E.J., 1984. Monte Carlo simulation of coagulation in discrete particle-size distributions. Part 1. Brownian motion and fluid shearing. J. Fluid Mech. 143, 367–385.

Saffman, P.G., Turner, J.S., 1956. On the collision of drops in turbulent clouds. J. Fluid Mech. 1, 16–30.

Sommerfeld, M., Zivkovic, G., 1992. Recent advances in the numerical simulation of pneumatic conveying through pipe systems. In: Hirsch, et al. (Eds.), Computational Methods in Applied Science First European Computational Fluid Dynamics, Brussels, pp. 201–212.

Sommerfeld, M., Kohnen, G., Rüger, M., 1993. Some open questions and inconsistencies of Lagrangian particle dispersion models. In: Proceedings of the Ninth Symposium on Turbulent Shear Flows, Kyoto Japan, Paper No. 15-1.

Sommerfeld, M., 1995. The importance of inter-particle collisions in horizontal gas–solid channel flows. In: Stock et al., D.E. (Eds.), Gas-Particle Flows, ASME, FED-vol. 228. pp. 335–345.

Sommerfeld, M., 1999. Inter-particle collisions in turbulent flows: A stochastic model. In: Banerjee, S., Eaton, J.K. (Eds.), Proceedings of the 1st International Symposium on Turbulence and Shear Flow Phenomena, Begell House, New York, pp. 265–270.

Sundaram, S., Collins, L.R., 1997. Collision statistics in an isotropic particle-laden turbulent suspension. Part 1. Direct numerical simulations. J. Fluid Mech. 335, 75–109.

Tanaka, T., Tsuji Y., 1991. Numerical simulation of gas–solid two-phase flow in a vertical pipe: On the effect of inter-particle collision. In: Stock et al. (Eds.), Gas–Solid Flows ASME FED-vol. 121, pp. 123–128.

Von Karman, T., Horwarth, L., 1938. On the statistical theory of isotropic turbulence. Proc. R. Soc. London, A164, pp. 192–215.

Wang, L.-P., Wexler, A.S., Zhou, Y., 1998. On the collision rate of small particles in isotropic turbulence I Zero-inertia case. Phys. Fluids 10, 266–276.

Williams, J.J.E., Crane, R.I., 1983. Particle collision rate in turbulent flow. Int. J. Multiphase Flow 9, 421–435.

Zhou, Y., Wexler, A.S., Wang, L.-P., 1998. On the collision rate of small particles in isotropic turbulence. II. Finite-inertia case. Phys. Fluids 10, 1206–1216.